AWARD NUMBER: **W81XWH-15-1-0628**

TITLE: **Targeting Dysregulated Epigenetic Enzymes for Prostate Cancer Treatment**

PRINCIPAL INVESTIGATOR: **Dr. David Jarrard**

CONTRACTING ORGANIZATION: **University of Wisconsin System**
Madison, WI 53715

REPORT DATE: October 2016

TYPE OF REPORT: Annual

PREPARED FOR: **U.S. Army Medical Research and Materiel Command**

Fort Detrick, Maryland 21702-5012

DISTRIBUTION STATEMENT: **Approved for Public Release;**

Distribution Unlimited

REPORT DOCUMENTATION PAGE

Form Approved
OMB No. 0704-0188

1. REPORT DATE	2. REPORT TYPE	3. DATES COVERED
October 2016	Annual	30 Sept 2015 - 29 Sept 2016

4. TITLE AND SUBTITLE
Targeting Dysregulated Epigenetic Enzymes for Prostate Cancer Treatment

5a. CONTRACT NUMBER

5b. GRANT NUMBER
W81XWH-15-1-0628

5c. PROGRAM ELEMENT NUMBER

6. AUTHOR(S)
David Jarrard, MD

E-Mail: jarrard@urology.wisc.edu

5d. PROJECT NUMBER

5e. TASK NUMBER

5f. WORK UNIT NUMBER

7. PERFORMING ORGANIZATION NAME(S) AND ADDRESS(ES)
University of Wisconsin System
21 N. Park St., Suite 6401
Madison, WI 53715

8. PERFORMING ORGANIZATION REPORT NUMBER

9. SPONSORING / MONITORING AGENCY NAME(S) AND ADDRESS(ES)
U.S. Army Medical Research and Materiel Command
Fort Detrick, Maryland 21702-5012

10. SPONSOR/MONITOR'S ACRONYM(S)

11. SPONSOR/MONITOR'S REPORT NUMBER(S)

12. DISTRIBUTION / AVAILABILITY STATEMENT
Approved for Public Release; Distribution Unlimited

13. SUPPLEMENTARY NOTES

14. ABSTRACT
This proposal provides an unbiased identification of aberrant enzymatic activities and histone PTM states in the development of castrate-resist PCa (CRPC). Using the peptide-microarray technology to obtain preliminary data, we found changes in hormone sensitive LNCaP and its castrate-resistant PCa clone CT-4 that identified several altered histone H3 acetyltransferases and deacetylases. We will apply this workflow t establish whether these enzymes are commonly dysregulated in other castrate-resistant PCa cell lines and in human PCa tissues, or whether distinct sets of epigenetic modifiers drive resistance in different patients. **Based on these data we hypothesize that specific histone-modifying enzymes altered during the development of castrate-resistant PCa (CRPC) can be targeted therapeutically.**
We propose 3 Specific Aims: *1*.) To identify dysregulated epigenetic enzymes in hormone-sensitive and CRPC, *2*.) To validate altered PTM states in human samples from hormone-sensitive and CRPC. *3*.) To provide proof-of–concept that CRPC is dependent on these aberrant enzyme activities and therefore responsive to small-molecules that target their activity. This novel study provides an unbiased identification of aberrant enzymatic activities and histone PTM states in CRPC. This understudied area in PCa is significant not only in identifying biomarkers for diagnosis and prognosis, but in providing a therapeutic strategy that targets epigenetic mechanisms.

15. SUBJECT TERMS
Peptide microarray, histone post-translational modification, epigenetics, prostate cancer, p300, lysine acetylation, deacetylation, Sirtuins, hormone-sensitive (HS), castrate-resistance (CR)

16. SECURITY CLASSIFICATION OF:			17. LIMITATION OF ABSTRACT	18. NUMBER OF PAGES	19a. NAME OF RESPONSIBLE PERSON
a. REPORT	b. ABSTRACT	c. THIS PAGE			USAMRMC
Unclassified	Unclassified	Unclassified	Unclassified	42	19b. TELEPHONE NUMBER *(include area code)*

Table of Contents

Page

Title: Targeting dysregulated epigenetic enzymes for prostate cancer treatment

1. Introduction

Prostate cancer (PCa) progression involves genetic alterations, but also dynamic epigenetic mechanisms resulting in gene expression changes critical for tumorigenesis. One major epigenetic process is the post-translational modification (PTM) of histone proteins, which wrap DNA and controls its accessibility for specific gene expression. There is growing evidence that dysregulation of enzymes that add or remove these PTMs is at the nexus of cancer initiation and progression. Therefore, new therapeutics for treating PCa lie in the identification of these aberrant enzyme activities and elucidating their role in PCa progression. To identify dysregulated chromatin enzymes, we have recently developed two novel methodologies. One approach utilizes a peptide-array technology to assay enzymatic activities on ~1000 unique histone peptides that differ in their sequence and PTM state. The second complementary approach is our recently developed LC-MS/MS method that allows simultaneous quantification of 60 histone PTM states from endogenous tissues and cells. This proposal provides an unbiased identification of aberrant enzymatic activities and histone PTM states in the development of castrate-resistant PCa (CRPC). Using the peptide-microarray technology to obtain preliminary data, we found changes in hormone sensitive LNCaP and its castrate-resistant PCa clone CT-4 that identified several altered histone H3 acetyltransferases and deacetylases. We will apply this workflow to establish whether these enzymes are commonly dysregulated in other castrate-resistant PCa cell lines and in human PCa tissues, or whether distinct sets of epigenetic modifiers drive resistance in different patients. **Based on these data we hypothesize that specific histone-modifying enzymes altered during the development of castrate-resistant PCa (CRPC) can be targeted therapeutically.** We propose 3 Specific Aims: *1*.) To identify dysregulated epigenetic enzymes in hormone-sensitive and CRPC, *2*.) To validate altered PTM states in human samples from hormone-sensitive and CRPC. *3*.) To provide proof-of–concept that CRPC is dependent on these aberrant enzyme activities and therefore responsive to small-molecules that target their activity. This novel study provides an unbiased identification of aberrant enzymatic activities and histone PTM states in CRPC. This understudied area in PCa is significant not only in identifying biomarkers for diagnosis and prognosis, but in providing a therapeutic strategy that targets epigenetic mechanisms.

2. Keywords

Peptide microarray, histone post-translational modification, epigenetics, prostate cancer, p300, lysine acetylation, deacetylation, Sirtuins, hormone-sensitive (HS), castrate-resistance (CR)

3. Accomplishments

Accomplishments Major Task 1: Identify dysregulated histone acetyltransferase (HAT) and deacetylase (HDAC) activities in Castration-Resistance Prostate Cancer (CRPC) cells and xenografts during progression from androgen dependence (AD).

Subtask 1: Measurement of endogenous acetylation and deacetylation activities in LNCaP and C4-2 cell lines (plus two additional AD/CRPC sets) and 5 LuCAP xenograft AD/CRPC sets by using histone peptide microarray assay. Statistical analysis for significance of microarray and to identify lysine acetylation sites displaying high divergence between the two cell lines.

Completed. We have performed this analysis in 5 cell lines and 12 xenografts. This information is included in the recently competed and submitted manuscript. (Figure 1-2, Figure 5 appendix) Further analyses are ongoing for other novel acetylation and deacetylation activities.

Subtask 2: Validation of the HAT activity from HTS histone peptide microarray analysis by time-course filter-binging HAT assays using synthetic histone peptides and radiolabeled 3H-AcCoA as substrates.

Completed. Included in manuscript (Figure 3 appendix).

Subtask 3: Validation of the sirtuin activity identified in the microarray result by in vitro biochemical method using a nicotinamide-dependent enzyme-coupled system.

Completed included in manuscript (Figure 4 appendix).

Subtask 4: Identification and validation of novel HAT and HDAC activities on specific targets
Completed for P300 and Sirt2 and data included in manuscript (Figure 4). Ongoing analysis of novel activities.

Milestone(s) Achieved:
-Identification and validation of novel HAT and HDAC activities on specific targets including P300 and Sirt2. Others identified and included in the attached submitted manuscript.

We developed a high-throughput peptide microarray assay to identify altered histone lysine (de)acetylation activity in prostate cancer (PCa). This microarray-based activity assay revealed up-regulated histone acetyltransferase (HAT) activity against specific histone H3 sites in a castrate-resistant (CR) PCa cell line compared to its hormone-sensitive (HS) isogenic counterpart.

NAD^+-dependent deacetylation assays revealed down-regulated Sirtuin activity in validated CR lines. Levels of acetyltransferases GCN5, PCAF, CBP and p300 were unchanged between matched HS and CR cell lines. However, auto-acetylation of p300 at K1499, a modification known to enhance HAT activity and a target of deacetylation by SIRT2, was highly elevated in CR cells.

Among all 7 Sirtuins, only SIRT2 and SIRT3 protein levels were reduced in CR cell lines.

Interrogation of HS and matched CR xenograft lines reveals that H3K18 hyperacetylation, increased p300 activity, and decreased SIRT2 expression are associated with progression to CR in 8/12 (66%).

Tissue microarray analysis revealed that hyperacetylation of H3K18 is a feature6 of CRPC. Inhibition of p300 results in lower H3K18ac levels and increased expression of androgen receptor.

Thus, a novel histone array identifies altered enzyme activities during the progression to CRPC and may be utilized in a personalized medicine approach. Reduced SIRT2 expression and increased p300 activity lead to a concerted mechanism of hyperacetylation at specific histone lysine sites (H3K9, H3K14, and H3K18).

Major Task 2: Demonstrate corresponding PTM state dysregulated in CRPC cells, xenografts, and human tissues compared to AD state.

Subtask 1: Sample preparations for endogenous histone extraction from the AD and CRPC sets including LNCaP and C4-2

Ongoing for 12 xenograft tumor sets as well as LNCaP and C4-2.

Subtask 2: Acquisition of LC-MS/MS data of samples prepared in 2.1. Quantitative analysis of specific histone modifications using Q-Exactive. Generate stable cell lines expressing plasmids developed in task 3.1

Planned.

Subtask 3: Western blot analysis of endogenous histone extraction from LNCaP and C4-2 cells/xenogafts/human tissues by probing with histone PTM-specific antibodies (sp. H3K9ac, H3K14ac, H3K18ac, and H4K20ac) that are relevant to CRPC and the result obtained in Task 1.

Planned

Milestone(s) Achieved: Demonstrate PTM state dysregulated in AD and CRPC cells/xenografts

Major Task 3: Identify histone modifying proteins (e.g. HATs and Sirtuins) that drive CRPC.

Subtask 1: Test for p300 inhibition using C646, in C4-2 cells and one or more transfectable CRPC cell line. Probe changes in acetylation.

Performed C646 inhibition and results reported in attached manuscript (Figure 5).

Subtask 2: Preparation of siRNA knockdown of p300 in C4-2 cell line and at least one other cell line. Evaluation of efficiency for siRNA knockdown by gene expression and western blotting.

Planned.

Subtask 3: Overexpression of Sirt6 in C4-2 cell lines using Sirt6-expression construct (previously prepared in the Denu lab). Analysis of Sirt6 expression.

Ongoing. Sirt6 expression was not downregulated in the C4-2 cell line with repeated studies. In contrast Sirt2, 3 and 4 were. Attached manuscript Figure 4.

Subtask 4: Time-course experiment for comparison of phenotypic behaviors (e.g. cell growth, apoptosis, senescence, acetylation levels on target genes, and gene transcript abundance) in 6 different samples; (1) WT LNCaP cells, (2) WT C4-2 cells, (3) C4-2 with p300 inhibition, (4) C4-2 with Sirt6 FA-activation, (5) C4-2 with p300 knockdown, and (6) C4-2 with Sirt6 overexpression.

Ongoing. Cell growth apoptosis and transcript alterations has been performed for P300 downregulation with C646 (Figure 5)

Subtask 5: Evaluation of additional statistically altered modifying enzymes identified in Task 1-2, using the similar workflow as described in 3.1-3.4. Assess if available small molecular inhibitors/preclinical agents against these enzymes.

Planned.

Milestone(s) Achieved: Confirmed that CRPC is dependent on these activities and test inhibitors as therapeutic approach using the agent C646. Further small molecule and novel drug studies planned.

Opportunities for training and professional development

These include post-doctoral student Dr Jin-Hee Lee who was the primary author of the completed study. Additional trainees include Nathan Damaschke a graduate student who performed the expression array analyses.

How were the results disseminated to communities of interest?

Submitted publication. Attached in appendix.

4. Impact

Emerging evidence indicates that targeting epigenetic mechanisms might provide a new paradigm for drug treatment in cancer. Increased HDAC activity in prostate tumors provides one target, and treatment with HDAC inhibitors (HDACi) such as Suberoylanilide Hydroxamic Acid (SAHA) and Phenylbutyrate (PB) induce pro-

apoptotic and growth inhibitory effects. In Phase I studies in advanced solid tumors including prostate biomarker evaluations have demonstrated an accumulation of acetylated histones and H4 indicating a target effect. A major hurdle with these approaches is a lack of selective targeting of modifications, a primary goal of the current proposal. We will use two new high-throughput assay platforms to identify different epigenetic states during the transformation from hormone-sensitive to CRPC. CRPC provides the initial target for this newer class of therapy given the focus of the PCRP on developing new effective treatments for men with high risk prostate cancer. Obtaining this information will permit us to be able to identify specific enzymes that are altered during PCa progression and examine *in vitro* and *in vivo* the effect of specific inhibitors of these enzymes on CRPC growth and viability. This will provide a rationale for the application of inhibitors, many that have been synthesized but not developed further, to patients overexpressing these enzymes in a personalized medicine approach. Finally, the identification of specific post-translational modifications associated with the development of CRPC may mark tumors at risk for progression to lethal disease permitting earlier intervention in these patients.

5. Changes Problems

Nothing to report.

6. Products

Jin-Hee Lee, Bing Yang, Nathan Damaschke, Melissa D. Boersma, Wei Huang, Eva Corey, David F. Jarrard, M. Denu. Identifying dysregulated epigenetic enzymes in the development of castrate-resistant prostate cancer. Cancer Research. Under review.

7. PARTICIPANTS & OTHER COLLABORATING ORGANIZATIONS

Senior key personnel have been working on the project since the initiation of the project with no changes.

The following individuals have worked on the project:

Name: David F. Jarrard, MD
Project Role: Principal Investigator
Researcher Identifier (e.g., ORCID ID):
Nearest person month worked: 1
Contribution to Project: David Jarrard has conceived and designed the study, reviewed all of the data and the analysis of all of the results on the project, wrote and revised the manuscript.

Name: John M. Denu, PhD
Project Role: Co-Principal Investigator
Researcher Identifier (e.g., ORCID ID):
Nearest person month worked: 1
Contribution to Project: John Denu has conceived and designed the study, reviewed all of the data and the analysis of all of the results on the project, wrote and revised the manuscript.

Name: Jin-Hee Lee, PhD
Project Role: Post-Doctoral Fellow
Researcher Identifier (e.g., ORCID ID):
Nearest person month worked: 0
Contribution to Project: Jin Lee has optimized the microarray-based enzyme assay platform, performed and analyzed the biochemical studies and immunoblot experiments, wrote and revised the manuscript. Funded through a DOD PCRP fellowship grant

Name: Bing Yang, MD & PhD
Project Role: Researcher
Researcher Identifier (e.g., ORCID ID):
Nearest person month worked: 4.6
Contribution to Project: Bing Yang has prepared all the PCa lines used in this study and performed the transcriptomic analysis on the cell lines and the mouse xenografts as well as cell inhibitor and other studies.

Name: Eric A Armstrong, MS
Project Role: Associate Researcher
Researcher Identifier (e.g., ORCID ID):
Nearest person month worked: 8.5
Contribution to Project: Eric Armstrong is performing the LC-MS/MS runs and sample prep, array interpretation and data monitoring.

Name: Nathan A. Damaschke
Project Role: Research Assistant
Researcher Identifier (e.g., ORCID ID):
Nearest person month worked: 0
Contribution to Project: Nathan Damaschke has analyzed human PCa cell line expression profile from GEO database repository and analyzed tissue microarray immunohistochemistry data. Funded through a training grant.

Has there been a change in the active other support of the PD/PI(s) or senior/key personnel since the last reporting period?
Yes, Dr. Jarrard has added the following new awards:

Principal Investigator name: David F Jarrard
Percent effort: 5%
Award Type and Number: n/a
Funding Agency/Institution: University of Wisconsin Igniter Award
Annual Direct Costs: $150,000
Total Award (Direct and Indirect Costs): $150,000
Project Period (start and end dates): 10/01/2014-9/30/16
Project Name: Development of epigenetic field effect biomarkers
Brief Project Description: This provides funding for the clinical development of a new prostate cancer biomarker.
Indicate if the project is related to the work proposed: No
If yes, indicate the project's relationship to the work proposed in this application:

Principal Investigator name: David F Jarrard
Percent effort: 15%
Award Type and Number: PC150332P2
Funding Agency/Institution: DOD
Annual Direct Costs: $180,000
Total Award (Direct and Indirect Costs): $826,200
Project Period (start and end dates): 4/1/16-3/31/19
Project Name: Fusion Genes Predict Cancer Recurrence
Brief Project Description: The objectives of the proposal are to validate and to determine if these fusion gene markers and the combined models predict clinical recurrence and short PSADT.
Indicate if the project is related to the work proposed: No
If yes, indicate the project's relationship to the work proposed in this application:

Principal Investigator name: David F Jarrard
Percent effort: 10%

Award Type and Number: PCR150221
Funding Agency/Institution: DOD
Annual Direct Costs: $125,000
Total Award (Direct and Indirect Costs): $573,750
Project Period (start and end dates): 4/1/16-3/31/19
Project Name: Synthetic Lethal Metabolic Targeting of Senescent Cells After Androgen Deprivation
Brief Project Description: The specific aims of this project are: 1) Determine whether ADT-metformin synergistic response is mediated via disruption of the Hsf1-mediated proteolytic stress response (PSR) , 2) Examine the synthetic lethal response involving ADT-metformin in vivo in cancers of variable androgen sensitivity and test marker of response and 3) Determine whether metformin combined with ADT results in improved cancer-specific survival and longer time to secondary interventions in patients on these agents. Indicate if the project is related to the work proposed: No
If yes, indicate the project's relationship to the work proposed in this application:

Principal Investigator name: David F Jarrard
Role: Principal Investigator
Percent effort: 15%
Funding Agency/Institution: DOD
Award Type and Number: PC150536
Annual Direct Costs: $184,841
Total Award (Direct and Indirect Costs): $3,013,865
Project Period (start and end dates): 4/1/16-3/31/19
Project Name: Functional and Molecular Diversity in the Tumor Microenvironment underlies Therapeutic Response and Resistance
Brief Project Description: The hypothesis for this project is that resistance to chemohormonal therapy in individuals newly diagnosed with prostate cancer results from 3 putative mechanisms, mutations in the androgen receptor, mutation in the DNA damage repair pathway and DNA damage associated secretory program in the stroma.
Indicate if the project is related to the work proposed No
If yes, indicate the project's relationship to the work proposed in this application

What other organizations were involved as partners?
Nothing to report

8. APPENDICES:

Jin-Hee Lee, Bing Yang, Nathan Damaschke, Melissa D. Boersma, Wei Huang, Eva Corey, David F. Jarrard, M. Denu. Identifying dysregulated epigenetic enzymes in the development of castrate-resistant prostate cancer. Cancer Research. Under review.

Title: Identifying dysregulated epigenetic enzymes in the development of castrate-resistant prostate cancer

Authors and affiliations.

Jin-Hee Lee[1,2], Bing Yang[3], Nathan Damaschke[3], Melissa D. Boersma[2,4], Wei Huang[5], Eva Corey[6], David F. Jarrard[3,7,8*], and John M. Denu[1,2,7*]

[1]Department of Biomolecular Chemistry, School of Medicine and Public Health, University of Wisconsin, Madison, WI.

[2]Wisconsin Institute for Discovery and the Morgridge Institute for Research, University of Wisconsin, Madison, WI.

[3]Department of Urology, School of Medicine and Public Health, University of Wisconsin, Madison, WI.

[4]Department of Chemistry and Biochemistry, Auburn University, Auburn, AL.

[5]Department of Pathology and Laboratory Medicine, School of Medicine and Public Health, University of Wisconsin, Madison, WI.

[6]Department of Urology, University of Washington, Seattle, WA.

[7]Carbone Comprehensive Cancer Center, University of Wisconsin, Madison, WI.

[8]Molecular and Environmental Toxicology Program, University of Wisconsin, Madison, WI.

Running title.

Aberrant acetylation identified by histone microarray assay

Précis.

Novel histone microarray assay employed to identify aberrant histone (de)acetylation in development of castrate resistant prostate cancer

Keywords.

Histone peptide microarray; histone (de)acetylation; prostate cancer epigenetics; castrate-resistance; and p300

[*]To whom correspondence should be addressed.

J. M. Denu, 2140 Wisconsin Institute for Discovery, 330 North Orchard Street, Madison, WI 53715, Phone: 608-265-1859, Fax: 608-316-4602, E-mail: john.denu@wisc.edu

D.F. Jarrard, 7037 Wisconsin Institute for Medical Research, 1111 Highland Avenue, Madison, WI 53792, Phone: 608-252-0937, Fax: 608-265-0614, E-mail: jarrard@urology.wisc.edu

Disclosure of Potential Conflicts of Interest

J.M.D. consults for Bio-Techne and FORGE Life Science.

ABSTRACT

There is a tremendous need for novel strategies aimed at directly assessing activities of histone modifiers to probe epigenetic determinants associated with disease progression. Here, we developed a high-throughput peptide microarray assay to identify altered histone lysine (de)acetylation activity in prostate cancer (PCa). This microarray-based activity assay revealed up-regulated histone acetyltransferase (HAT) activity against specific histone H3 sites in a castrate-resistant (CR) PCa cell line compared to its hormone-sensitive (HS) isogenic counterpart. NAD^+-dependent deacetylation assays revealed down-regulated Sirtuin activity in validated CR lines. Levels of acetyltransferases GCN5, PCAF, CBP and p300 were unchanged between matched HS and CR cell lines. However, auto-acetylation of p300 at K1499, a modification known to enhance HAT activity and a target of deacetylation by SIRT2, was highly elevated in CR cells. Among all 7 Sirtuins, only SIRT2 and SIRT3 protein levels were reduced in CR cell lines. Interrogation of HS and matched CR xenograft lines reveals that H3K18 hyperacetylation, increased p300 activity, and decreased SIRT2 expression are associated with progression to CR in 8/12 (66%). Tissue microarray analysis revealed that hyperacetylation of H3K18 is a feature of CRPC. Inhibition of p300 results in lower H3K18ac levels and increased expression of androgen receptor. Thus, a novel histone array identifies altered enzyme activities during the progression to CRPC and may be utilized in a personalized medicine approach. Reduced SIRT2 expression and increased p300 activity lead to a concerted mechanism of hyperacetylation at specific histone lysine sites (H3K9, H3K14, and H3K18).

INTRODUCTION

Histone post-translational modifications (PTMs) including acetylation, methylation, and phosphorylation exist in highly specific and combinatorial fashion, impinging upon other epigenetic marks and influencing specific transcriptional regulation (1-3). Dysregulated histone modifications alter intrinsic chromatin structure as well as the surface architecture, leading to erroneous recruitments of gene regulatory machineries at specific genomic loci (4). Therefore, altered cellular abundance and activity of histone modifiers is thought to play a key role in cancer progression.

Many PTMs are reversible and in dynamic interaction with antagonistic enzyme activities. A systematic interrogation of aberrant enzyme activities leading to distinctive histone PTM patterns would be crucial to understanding the molecular mechanism by which particular disease states are established. Such knowledge is essential for developing therapeutics to target these enzymes. Recent advances in genomic and proteomic data mining tools together with Chromatin Immunoprecipitation (ChIP)-based profiling have been instrumental in unraveling aberrant expression of histone-modifying complexes in specific disease progression (5-8). However, post-transcriptional, -translational regulation, and longevity of gene products poorly correlates with genome-wide transcript levels and their protein amounts (9). Furthermore, protein PTM, subcellular targeting, and the level of small molecule activators or inhibitors make it difficult to directly link protein levels with their biological activities (10). Hence, there is tremendous need for novel strategies aimed at directly assessing activities of histone modifiers as an alternative and complementary avenue for probing epigenetic determinants associated with disease progression.

Prostate cancer is the most commonly diagnosed disease in American men, and 30,000 die annually primarily due to progression of the disease to its CR forms (11). After an initial response to hormone ablation therapy, metastatic HS cancers relapse and progress to CRPC (12). Targeting the molecular determinants of this event would be pivotal for developing new prognostic and therapeutic strategies. Previous studies report that global levels of several histone modifications including

H3K18ac and H3K4me2 are associated with PCa tumor recurrence suggesting a role for histone modifications in cancer progression (13,14). Isolated histone-modifying enzymes have been found to have impaired activity in various cancers (15,16), however, a systematic evaluation of aberrant epigenetic enzyme activity in the progression to CRPC is lacking.

In this study, we examine dysregulation of global (genome-wide) lysine (de)acetylation activities during PCa progression by utilizing novel peptide microarray technology in cell extracts from relevant cancer models and human tissues. Previously, we had demonstrated utility of peptide microarrays for identifying targets of chromatin "reader" proteins against combinatorial histone PTMs in a high-throughput protein binding assay (17). Here, we prepared histone peptide libraries consisting of 932 unique peptides covering human histone H3, H4, H2A, and H2B sequences of different histone variants. This library includes combinatorial histone PTMs likely to be found in human chromatin (18), allowing interrogation of HAT and histone deacetylase (HDAC) activities in cell lysates from CR versus HS cells. Validating these microarray-identified differential activities using quantitative immunoblot analysis revealed corresponding differences in histone marks in PCa cells. Based on these results and an expanded analysis, we identified several putative HATs and HDACs associated with these altered activities, not previously described, in PCa progression to CR. Thus, peptide microarrays-based analysis of chromatin modifying enzymes is a useful approach to identify dysregulated activities associated with cancer progression and we anticipate it can be utilized in a personalized medicine approach to disease treatment.

MATERIALS and MEHODS

Preparation of Histone Peptide Microarray. Peptides (13 amino acids) were synthesized on modified cellulose discs (celluspots) with a ResPepSL automated synthesizer (Intavis AG, Köln, Germany) via standard Fmoc/tBu chemistry as previously described in Su *et al* (17). Each synthesis included peptide with an acid cleavable linker for quality assessment by HPLC and mass

spectrometry. Peptide side chains were cleaved and the cellulose peptide conjugates were dissolved, extracted, diluted and aliquoted into 384-well polypropylene plates for printing. Gene Machines OmniGrid Arrayer (Genomic Solutions) with TeleChem SMP3 quill-like pins was used to contact-print the cellulose peptide conjugates onto the 75 mm × 25 mm nitrocellulose slide (Intuitive Biosciences). Each array housed duplicate sets of the peptide library ("subarrays"), allowing two reaction conditions to be probed on the same slide. Each subarray is arranged into 18 blocks made up of 13 rows × 13 columns of spots, permitting a spatial arrangement of 169 spots per block (i.e. 6,084 spots per each slide). 932 histone peptides which make up our histone library were printed in triplicate. Positive control spots consisted of acetyllysine(K_{ac})-containing peptides and negative control spots were cellulose without any peptide conjugation or peptides without any Lys residues. The control spots were included in every block design, each printed by a same printing pin of the OmniGrid Arrayer. Fluorescent Cy3 dye (Lumiprobe Life Science Solutions) was conjugated to cellulose, and mixed to each peptide stock solution to serve as spot tracer (green, 532 nm), while peptides carrying K_{ac} PTM fluoresced at 635 nm (red). Once the peptides were spotted, the slide was dried overnight at RT and stored at 4°C until use.

Microarray Enzyme Activity Assay and Data Analysis. All the microarray assays were performed with a multi-chamber simplex gasket (Intuitive Biosciences), which allows multiple reaction conditions for each array. All the buffers used in the assay were filtered prior to use, and peptide arrays were protected from light at all times. Rubber gaskets were thoroughly washed with 70% EtOH and completely dried prior to each assay. Each array was blocked with 2% bovine serum albumin (BSA) in TBST at 4°C overnight to eliminate non-specific protein binding to the nitrocellulose surface. Following blocking, each chamber was filled with reaction buffer; 20 mM Tris-HCl (pH 7.5), 1 mM DTT supplemented with Trichostatin A (TSA, HDAC inhibitor), protease inhibitor cocktail (Promega), and NaF (phosphatase inhibitors). For HAT-specific assays, 50 μM

acetyl-CoA and 5 mM nicotinamide (Sirtuin inhibitor) were supplemented, while for Sirtuin deacetylation assays, 50 μM NAD^+ and 2 mM anarcardic acid (HAT inhibitor) were added. In each chamber was added nuclear extract from each cell type. Unless otherwise noted, all the chemicals were obtained from Sigma-Aldrich. After the array was incubated at 25°C for 1 hour, the reaction was stopped as the assay components were removed by gentle aspiration. The array was washed with TBST before incubated with rabbit-derived *pan*-K_{ac} antibody (Cell Signaling Technology). After washing off the unbound antibody, the slide was incubated with *anti*-rabbit IgG conjugated to Alexa647 (Cell Signaling Technology). The slide was washed with TBST multiple times before scanned on an Axon GenePix 4000B microarray fluorescence scanner (Molecular Devices) at 5-μm pixel resolution and 33% laser power. Slide images were collected at 532-nm/635-nm dual channel, and analyzed using GenePix Pro 6.1 software (Molecular Devices). For alternative detection of HAT assays, isotopic incorporation of acetyl group from a trace amount of radiolabeled ^{14}C-acetyl-CoA (2.5 μCi, Moravek Biochemicals) was performed. Once the reaction was complete, the array was washed three times with TBST, followed by a final wash with filtered Milli-Q water, and allowed to dry. The array was exposed to BAS-IP TR2015 tritium screen (Molecular Dynamics) for 1 week at room temperature. The transferred phorphorimage was scanned at 10 μm pixel resolution on a Typhoon FLA 9000, and analyzed under a fixed spot area quantification by ImageQuant TL software (GE Healthcare).

For GenePix data analysis of *pan*-K_{ac} antibody detection, total signal intensity of both Alexa647 (635 nm) and Cy3 (532 nm) were utilized. The spot quality was evaluated via visual inspection of the tracer dye for any signs of artifacts during printing, i.e. missing or distorted spots, or spots with “tadpoles” (Supplementary Fig. S1). Additionally, spots that do not meet the following requirements were filtered off during preprocessing. First, any spots with mean intensity at 532 nm less than 10% of averaged total mean intensity was considered ‘printing error’ or ‘blank’ and was no further considered. Second, each technical replicate was subjected to Grubbs test and outliers from a

normal distribution were eliminated. In general, with 0.1% risk of false rejection applied (at $n = 3$; $G_{critical}$, 1.1547), greater than 99% of total population remained within the confidence interval. Global normalization for total intensity was applied to adjust systematic variation. The differential K_{ac} signal was measured as the $\log_2$ (ratio of K_{ac} intensity in C4-2 over K_{ac} intensity in LNCaP) and reported as a mean of three independent microarray assays performed with biological replicates. The microarray design and the list of peptides in the histone library are provided in Supplementary Table S1-S2.

$$G = \frac{|x_i - x_{avg}|}{s}$$

Studies with Human Cell Lines and Mouse Xenograft. LNCaP, C4-2, LAPC4 and 22RV1 cells were cultured in DMEM media (Corning cellgro) containing 1 g/L glucose, L-glutamine, and sodium pyruvate, 10% fetal bovine serum (FBS) and 1% penicillin/streptomycin. PC3 and DU145 were cultured in DMEM media (Corning cellgro) containing 4.5 g/L glucose, L-glutamine, and sodium pyruvate, 10% FBS and 1% penicillin/streptomycin. All cell lines were incubated at 95% air; 5% carbon dioxide at 37°C. Each cell line was cultured from one 100 mm plate (approximately 1×10^7 cells each). Harvested cells were flash-frozen and stored at -80°C for a maximum of 3 months. Each cell pellet was thawed on ice and resuspended in 300 µL lysis buffer; 50 mM Tris-HCl, pH 7.5, 150 mM NaCl, 1% Triton X-100, DNase I (Roche), protease inhibitor cocktail (Promega), and NaF and incubated at room temperature for 10 min with gentle rotation. The cell suspension was passed through 27-gauge needle 10 times, and the lysate was centrifuged at 14,000 g for 5 min at 4°C.

For mouse xenograft study, 12 pairs of each HS and CR human prostate tissue were prepared. LuCaP patient-derived xenografts were grown subcutaneously in intact (HS lines) and castrated (CR lines) SCID male mice (19). RNA was isolated from the tissues using Perfect Pure RNA Tissue Kit (5-Prim) following the protocol supplied by the manufacturer. DNase I was used to digest RNA to eliminate any contaminating genomic DNA. cDNA was synthesized with qScript cDNA superMix (Quanta Biosciences) using 1µg of total RNA with both Oligo(dT)s and Random

Haxamer Primer present. To further eliminate gDNA contamination, the amplification of cDNA are achieved by designing exon-primed intron crossing primers, in which the forward and reverse primers flank at different exons. qPCR was performed using a CFX96 real-time PCR (Bio-Rad), Perfecta Sybr green fast-mix (Quanta Biosciences) to measure gene expression. For all expression experiments, GAPDH is used for housekeeping gene. Information to antibodies and the protocol used for preparing cell extracts and western blot analysis is in the Supplementary Materials and Methods.

Histone PTM Assays. Recombinant full-length histone (*Xenopus laevis*), H2A and H3, used in the enzyme assay was expressed in BL21(DE3)pLysS and purified according to the Luger *et al* (20). Histone peptides that were not cellulose-conjugated were synthesized by Fmoc-based peptide synthesis (University of Wisconsin Peptide Synthesis Facility), and purified on a C18 column by Beckman BioSys 510 HPLC. *N*-terminally His_6-tagged PCAF (human), piccolo NuA4 (yeast), and SIRT2 (human) were overexpressed in BL21(DE3), and purified on a Ni-charged HiTrap HP affinity column (GE Healthcare). All the recombinant enzymes used in the pilot experiments were purified to near homogeneity and were tested for their specific activities against histone protein substrates. For measuring HAT activity of purified recombinant HATs as well as that in nuclear extracts, filter-binding assay was used as previously reported (21).

Immunohistochemical Staining of Tissue Microarrays. A tissue microarray containing 18 HS and 18 CR cancer tissues in quadruplicate was obtained from the Prostate Cancer Biorepository Network. Slide preparation and image analysis were conducted as previously described (22). Briefly, 5 μm sections were taken through routine deparaffinization and rehydration. One triple stain (H3K18ac, SIRT2, and E-cadherin) and one double stain (p300, E-cadherin) were performed from two TMA sections. Information on the primary antibodies used in this experiment is available in Supplementary Materials and Methods. E-cadherin antibody was used to define the epithelial compartment for

automated tissue segmentation. Stained slides were scanned using VECTRA (PerkinElmer, Waltham, MA) as previously described (22). Cores with <5% epithelial component or tissue loss were excluded from the analysis. InForm 1.2 software (PerkinElmer, Waltham, MA) was used to segment tissue subcellular compartments and tissue compartments. Epithelial staining intensity automatically quantified using inForm software was used for analysis of protein expression. Quadruplicate cores were averaged for a more precise estimate of protein expression. Tissues were required to have at least two cores with sufficient epithelium and tissue to be included in analysis.

C646 p300 Inhibition. mRNA expression of AR and PSA in prostate cancer cell lines LNCaP (HS), and DU145 (CR) were measured after treating with C646 (p300 inhibitor). The cell lines were treated with C646 at the concentration of 2.5, 5 μM. For control experiment DMSO was substituted for C646. After 1 h, and 48 h, cells were harvested, and RNA was isolated from the cells using Perfect Pure RNA Tissue Kit (5-Prism) following the manufacturers protocol. Same mRNA measurement procedure as described in the SIRT2 mRNA measurement (previous section) was used. The expression was normalized by GAPDH, and the data is shown as relative expression mean ± s.d. The list and sequence of primers used in this study is provided in the Supplementary Table S4.

Statistical Analysis. Data are shown as a mean ± s.d. with minimum *N o*f three replicates unless otherwise noted. All the graphs were generate using Prism (GraphPad software) except for the tissue microarray immunostaining which was generated using R package (Bioconductor; ggplot2). Student's t-test was used to determine the significance of the differences between two groups. $P< 0.05$ was considered significant.

RESULTS

Development and Validation of Histone Peptide Microarray for HAT and Sirtuin Assays

The primary goal was to establish a microarray-based enzyme assay that could detect subtle changes in the activities of chromatin modifying enzymes from cells. Initially, we developed a microarray enzyme assay to detect changes in the acetylation status of hundreds of immobilized histone peptides that are either synthetically acetylated or unmodified. The peptides were prepared as cellulose conjugates by the SPOT synthesis (23), and were printed on nitrocellulose-coated microscopic slides. Its high-binding capacity and relatively low fluorescence background make nitrocellulose an excellent choice for fluorescent detection of peptides when monitoring enzymatic activity (24). Changes in the acetylated lysine (K_{ac}) state were quantified by utilizing a "pan-specific" *anti*-K_{ac} antibody which is routinely used for enrichment of acetylated peptides in mass spectrometry-based analyses (25). Adopted from immunodetection methods, antibody-bound peptides are identified using an AlexaFluor®647-tagged secondary antibody (Fig. 1A). AlexaFluor®647 emits red fluorescent light upon excitation at 635 nm and serves as a measure of the presence of K_{ac}. We incorporated a second green Cy3 tracer dye (532 nm) in all peptide stock solutions, effectively creating a dual-channel detection system for quality control (Fig. 1B, Supplementary Fig. S1). The green signal facilitates peptide spot recognition for quantification, and also serves to identify any printing errors that are not uncommon when arraying large libraries (Supplementary Fig. S1).

We examined the reproducibility of signal responses to antibody detection between the peptides in each subarray after treating them separately using a duplex assay chamber. The signal intensity of each peptide between subarrays exhibited high inter-subarray concordance as represented by scatter plots with strong positive correlation (Fig. 1C). Coefficients of variation (CV) as a function of signal intensity (F_{635}) across three technical replicates of 997 peptides (including controls) were low (mean = 4.2%, median = 2.6%), and > 98% of detectable peptides showed CV not greater than 20%. Together with the high correlation between subarrays, the low technical variability was a strong

indication that this microarray assay platform can be used with high confidence. Dynamic range of *anti*-pan-K_{ac} antibody reflected a linear increase of signal intensity in response to the increased number of acetylated lysine residues per peptide (*n*), as represented in a box-and-whisker plot (Fig. 1D). Low percentage of false positives (< 5% of 711 peptides) and false negatives (< 3% of 218) were observed. The difference in signal intensity among the same *n* group is in part caused by variable affinities of the *anti*-pan-K_{ac} antibody towards each peptide's distinctive epitope (with different sequences and PTMs flanking an K_{ac} site) as well as by slight concentration differences in peptide stock solutions. This assay is, therefore, best utilized to determine changes in the HAT and HDAC activity levels between samples.

To investigate if HAT-dependent lysine acetylation can be evaluated on the peptide microarray platform, we utilized recombinantly expressed and purified HATs with unique substrate specificity. In this pilot assay a mini-library consisting of sixteen peptides was probed in a multiplex assay chamber allowing multiple assay conditions to be tested simultaneously on a single array (Supplementary Fig. S2). Addition of acetyl group was detected by phosphor imaging of [^{14}C]-acetyl moiety transferred from [^{14}C]-acetyl-CoA to peptide lysine. In this radio-isotopic detection, NuA4 displayed HAT activity toward peptides corresponding to the *N*-terminal H4 sequence, while showing no detectable activity towards *N*-terminal H3 peptide or globular regions of H4. Similarly, fluorescence immunodetection of acetyllysine using *pan*-K_{ac} antibody revealed that lysine acetylation was HAT-dependent, consistent with the substrate specificity of both NuA4 and PCAF reported previously (26,27). The two independent detection methods yielded consistent results. Peptides containing synthetically installed K_{ac} (positive controls) produced positive signals while peptides lacking lysine residue (negative controls) did not exhibit measurable fluorescent signal. When used in this mini-library with peptide spots larger than 200 μm in diameter, quantification by isotopic detection was feasible. While isotopic detection can eliminate issues associated with a few false positive signals caused by antibody cross-reactivity, the antibody-based method exhibits better spatial

resolution and higher signal sensitivity. Thus we chose the antibody-based method for the subsequent large library screening.

To examine deacetylation activity in the microarray format, we performed pilot assays with NAD^+-dependent Class III HDACs, known as Sirtuins (28). Here we employed recombinantly expressed Sirtuins 1-3, and co-incubated with NAD^+ co-substrate. Sirtuin-dependent deacetylation was prominent, while non-enzymatic deacetylation was negligible (Fig. 1E). To evaluate whether endogenous enzymatic activity can be measured in these peptide arrays, we repeated the experiments with whole-cell extracts from HEK293T cells. Inhibitors of phosphatase, protease, HDAC (I, II) and HAT activity were included to prevent any complicating modifications (other than deacetylation by Sirtuins) that can result in K_{ac} signal change. In HEK293T cell extracts without added recombinant Sirtuins, the K_{ac} signal was reduced by up to 40%, suggesting endogenous Sirtuin activity can be captured by this microarray assay. When cell extracts were supplemented to the recombinant Sirtuins, the deacetylation activity was slightly reduced, suggesting presence of proteins or small molecules that may occupy and compete for the specific deacetylation sites. Overall, the favorable results of the pilot HAT and Sirtuin assays indicate that this novel microarray platform is compatible for enzyme activity assays using recombinant enzymes and cell lysates.

Differential Histone Acetylation in Prostate Cancer Cells (LNCaP versus C4-2)

Next we investigated whether dysregulated activities of histone modifying enzymes, HATs and Sirtuins, are present during progression of the HS cell line, LNCaP, to its CR daughter cell line, C4-2 (29). The LNCaP and C4-2 PCa model system follows phenotypic behavior similar to clinical models providing a unique opportunity for studying PCa progression in cell lines (29,30). Using cell extracts, we adopted similar assay conditions used in the pilot enzyme study, and compared the resulting K_{ac} signals in one subarray treated with LNCaP cell lysate to that in the second subarray treated with C4-2 lysate (Fig. 1F). In the HAT specific assay, acetyl-CoA, TSA (HDAC inhibitor),

and nicotinamide (sirtuin inhibitor) were supplemented in addition to protease and phosphatase inhibitors. In the Sirtuin-specific assay, NAD^+, TSA, and anarcardic acid (HAT inhibitor) were added while acetyl-CoA was excluded. After each experiment, the peptide array was processed and the data analyzed. The K_{ac} signals were determined and presented as $\log_2$ of C4-2 signal over LNCaP signal. For each biological replicate, cells were grown separately and lysed individually.

Figure 2 summarizes the representative histone peptides having the highest K_{ac} signal difference between LNCaP and C4-2. With the HAT activity assays, C4-2 displayed increased acetylation on the *N*-terminal (amino acids 1-20) lysines of H3 peptides in the order of K18, K4, K9, and K14, while there was reduced relative K_{ac} signals in H3K79 and H2A K13/K15 in C4-2 compared to LNCaP (Fig. 2A). For the Sirtuin activity assay, we observed higher Sirtuin activity on the H3K122ac and H3K56ac in C4-2, while there was lower activity on the H3K9ac, H3K14ac, and to lesser extent on the *N*-terminal lysines of H4 (Fig. 2B). Most up-regulation (positive log2) in HAT activity or down-regulation (negative log2) of Sirtuin activity in C4-2 took place on the same histone lysine residues, leading to marked combined effects on K_{ac} status. For instance, up-regulation in HAT activity against H3K9 was observed while Sirtuin assays revealed decreased deacetylation activity on H3K9ac, leading to potential net increase in H3K9ac signal. Increased K_{ac} signals are shown as blue bars while red bars represent decreased K_{ac} signal. Overall, the net effect on the K_{ac} signal changes in peptides containing H3K9, H3K14, and H3K18 were most prominent and these PTMs were investigated in the following experiments.

To validate the microarray results, we performed a highly sensitive in-solution HAT assay and demonstrated that the differential histone acetylation at specific lysine sites could be confirmed by independent methods (Fig. 3). An H3 histone peptide (aa 1-20) bearing the lysine sites with the highest differential activity (K4, K9, K14, and K18 of histone H3) were co-incubated with ^{3}H-acetyl CoA and extracts from either C4-2 or LNCaP cells. Incorporation of radioactive acetyl group on the histone peptide was quantified by scintillation counting. The results revealed a 55% higher rate of

HAT activity in the C4-2 cells compared to the LNCaP cells after 2 h incubation at 30 °C (Fig. 3A). Both LNCaP and C4-2 exhibited increased acetylation over time, while none of the controls that lacked either cell extracts or substrate peptide showed signs of increased acetylation.

The enzyme assays clearly indicate that C4-2 cells display higher HAT activity and lower Sirtuin activity on several overlapping lysine residues. To investigate whether these dysregulated activities represent true cellular dysfunction between C4-2 and LNCaP cells, we investigated the site-specific acetylation levels (immunoblots) on histone extracted directly from each cell line. We predicted that differential (de)acetylation activity observed in the microarray assay should be reflected in the acetylation status of endogenous histones. Western blot analysis was focused on three of the "top hits" revealed in the microarray data. Consistent with the microarray and in-solution assays, the levels of endogenous acetylation at H3K9, H3K14, and H3K18 in C4-2 cells were elevated compared to LNCaP (Fig. 3B). Increases in the level of H3K9ac and H3K18ac at the global level reached statistical significance, while the increase in H3K14ac level did not. Together, these results confirm the utility of our microarray analysis in detecting specific difference in the chromatin modifying activities found among highly related cancers.

Endogenous Protein Levels of HATs and Sirtuins

An important feature of the microarray assay is the ability to detect differences in enzymatic activity even when comparisons of proteins levels in western blots (or comparable ELISA) reveal no significant changes. To identify putative enzymes responsible for the altered (de)acetylation activities, we first investigated the endogenous protein levels of particular HATs that affect H3 acetylation. These HATs include p300/CBP that regulates gene expression by acetylation of histone and other transcription factors, and are reported to be more promiscuous with respect to substrate sequence recognition (31). Other putative HATs include the GNAT family, GCN5 and PCAF. No significant changes were detected in the level of GCN5, PCAF, and p300 by immunoblotting (Fig.

4A). The possibility that a PTM-regulated mechanism is involved therefore merited investigation. P300 undergoes autoacetylation at amino acid residue K1499 which results in enhanced HAT catalytic activity (32), so we performed western analysis to detect endogenous amount of acetyl-p300 (K1499ac), which revealed a marked increase in C4-2 compared to LNCaP (Fig. 4A). Collectively, these observations suggest that increased HAT activity in C4-2 can be attributed to activated, acetylated p300.

Next, we investigated the protein levels of the 6 Sirtuins (SIRT1-4, 6, and 7) in C4-2 and LNCaP cells to assess whether altered protein expression of a specific Sirtuin enzyme was responsible for the overall lowered NAD^+-dependent deacetylation observed in the C4-2 cells. Quantitative immunoblot analysis revealed that among the 6 Sirtuins, only SIRT2 and SIRT3 displayed significant loss of protein expression during the transition from LNCaP to C4-2 (Fig. 4B). SIRT3 is a mitochondrial enzyme, while SIRT2 is known to function in the nucleus and the cytoplasm. Most importantly, SIRT2 was shown to regulate the acetylation level of the activated form of acetyl-p300 (K1499ac) (33). The combined observations of acetylated, hyperactive p300, and loss of SIRT2 expression in the C4-2 cells suggests that the dramatically decreased protein levels of SIRT2 leads to the inability to down-regulate the hyper-acetylated form of p300.

SIRT2-dependent deacetylation of p300, and SIRT2 expression in PCa cell lines and human tissue

To further establish the link between hyperacetylated activated p300, and decreased Sirtuin activity in the CR cell line C4-2, we performed an *in vitro* NAD^+-dependent deacetylation assay using cell extracts from both LNCaP and C4-2 cells with or without recombinant SIRT2 (Fig. 4C). Addition of NAD^+ to C4-2 cell extracts was not sufficient to completely remove acetyl modification from p300, while addition of both SIRT2 and NAD^+ led to a loss of immunoreactivity against acetyl-p300 (K1499ac). Consistent with the protein abundance of acetyl-p300 (K1499ac) observed from

immunoblot (Fig. 4A), LNCaP cells displayed lower acetylation at K1499 whether or not NAD^+ was added (Fig. 4C). Next we examined whether SIRT2 and SIRT3, the only Sirtuins significantly lower in C4-2 compared to LNCaP were altered in extracts from HS cells (LAPC4, and LNCaP) and CR cells (PC3, DU145, 22RV1, and C4-2). Lower levels of both proteins in CR cells relative to the two HS PC cell lines were seen (Fig. 4D). Consistent with this observation, analysis of gene expression data obtained from NCBI Gene Expression Omnibus (GEO) data depository for prostate cancer cell lines indicate that there is a statistically significant downregulation of SIRT2 and SIRT3 expression in CR cell line DU145 when compared to the HS LNCaP cells while p300 gene expression data showed the levels of p300 remains unaltered between LNCaP and DU145 (Supplementary Fig. S3A-C).

Using a well-described human xenograft model system (19), we interrogated the SIRT2 mRNA expression in matched human tumors before and after the development of CRPC. We observed that in the majority of CR samples (7 out of 12 sets; 58%), SIRT2 expression was downregulated when compared to its HS paired precursor (Fig. 5A). Collectively, these data indicate that reduced expression of SIRT2 is associated with the development of CR in the majority of human tumors directly assessed during progression.

Having shown that loss of SIRT2 expression, increased p300 activity and histone H3 hyperacetylation are associated with the transition to CR, we next examined a unique tissue microarray to determine whether any of these observations were evident amongst a series of HS and CRPC samples of human PCa tissue (34). The arrays were analyzed and quantified for protein abundance of p300, H3K18ac and SIRT2 using VECTRA automated analysis (Fig. 5B). Acetyl-p300 (K1499) protein levels were not examined due to antibody limitations. P300 levels trended lower in HS compared to CRPC tissues with broad expression patterns noted in the CRPC group ($p = 0.075$) (Fig. 5C). However, CRPC showed a marked increase in K18ac ($p = 0.013$) compared to the HS tumors. SIRT2 expression was highly variable in both groups ($p = 0.56$), with 8/15 (45%) of CPRC

specimens demonstrating lower expression than the HS mean (Fig. 5C). These specimens were not matched with regard to progression in individual patients.

Inhibition of p300 activity has previously been demonstrated to decrease the proliferation of PC3 and other CR prostate cancer cell lines when exposed to the inhibitor C646 (35), a response we confirmed (data not shown). To confirm the dependency of H3K18ac on p300 activity in these lines, exposure to C646 resulted a consistent decrease in H3K18ac levels (Fig. 5D). Finally, to further investigate this phenotype after p300 inhibition, LNCaP and PC3 cell lines were exposed to C646 and an increase in androgen receptor (AR) and its target PSA were seen in the AR negative DU145 cell line (Fig. 5E). No increase was seen in the LNCaP line already robustly expressing these genes. Taken as a whole, evaluation of cell lines, xenografts and tissue microarrays implicates the SIRT2 and p300/CBP in dictating the CR PCa transition in chromatin dynamics and transcription.

DISCUSSION

High-throughput approaches to discover critical histone modifying enzymes during cancer progression offer a unique approach to improving cancer therapy strategies. For the first time, histone peptide microarrays were used to quantify differential lysine acetylation and deacetylation activities during the progression to castrate resistance in PCa cells. Covering the entire human histone sequences with prevailing combinatorial PTMs, we show that the site-specific acetylation and deacetylation activities can be resolved reliably with high sensitivity when comparing two conditions. Indeed, our screening of two cells lines (C4-2 vs. LNCaP) of the same genetic origin uncovered dysregulated acetyl-p300 and SIRT2. Thus, such microarray-based enzymatic assays can be successfully employed as a discovery tool to reveal novel mechanisms by which histone-modifying activities might drive the epigenetic landscapes to pathological states.

P300 is autoacetylated on multiple lysine sites by an intermolecular mechanism and one of these sites K1499 is critical for enhanced HAT activity (32,36). It was previously reported that

deacetylation of p300 at K1499ac is SIRT2-dependent (33). Our unbiased histone array assays detected increased HAT and decreased NAD^+-dependent deacetylase activities against specific lysine sites in histones. Strong activation of H3K18 acetylation occurred in CRPC tissues compared to HS primary and metastatic tissues in the unique series of tissue arrays tested (Fig 5). SIRT2 expression was not uniformly decreased in all CRPC samples tested, but SIRT2 functional mutations have been recognized (37), and activity may also be altered through other posttranslational mechanisms (38). Follow-up experiments strongly suggested that these activities could be assigned to activated p300 and reduced SIRT2/3. Taken together, the results suggest that loss of SIRT2 expression (activity) in some CR cells leads to uncontrolled activation of autoacetylated p300, which has been previously linked to CR gene-expression (39).

While this mechanism is likely, it is important to point out that we observed decreased ability of C4-2 cell extracts to catalyze the NAD^+-dependent deacetylation of H3K9, H3K14, H3K18, which are targets of p300/CBP and SIRT2. Thus, while K1499ac is a target of SIRT2, the observed endogenous hyperacetylation of H3K9, H3K14, H3K18 could be the result of SIRT2 loss or increased p300/CBP activity or both. Adding to the p300/CBP-SIRT2 connection, it has been reported that p300 acetylates SIRT2 to attenuate its deacetylation activity (40). SIRT2 and p300 have multiple layers of antagonizing activities that would be entirely consistent with the majority of trends observed in the cell lines, xenografts and tissue microarray. Previous studies have shown a close link between SIRT2 expression and suppression of tumorigenesis (41,42). To our knowledge no direct evidence has been reported to date whether SIRT2 affects the progression to CRPC. Expression of SIRT2 in PCa cells has not been examined, although deacetylation of α-tubulin, which is SIRT2-dependent, was shown to be up-regulated in CR PCa cell PC3 (43). Furthermore, recent data suggests SIRT2 plays a role as a mitotic checkpoint, maintaining genomic integrity (44), and impairing cell motility through perturbation of microtubule dynamics (45,46).

In this novel unbiased analysis of histone modifying enzymes, we have uncovered a distinct molecular pathway in progression to CRPC in which SIRT2 appears to play an important role. This has potential to be utilized in a personalized medicine approach to direct therapy against altered enzymes with further development. A variety of new inhibitors targeting histone modifying enzymes are being developed offering new options for cancer treatment (47). Other enzyme alterations strongly supported by our study include SIRT3, which deserves further investigation. In addition, other dysregulated activities identified in our microarray study include deacetylation at H3K56ac. The enzyme responsible for this modification is SIRT6, of which the cellular protein abundance remained unchanged in our study, however, there remains the possibility SIRT6 catalytic efficiency is affected in a similar fashion as in SIRT2-p300 cross-talk mechanism. While this speculation lends further supports, together these results provide proof-of-concept for the unbiased use of our histone array assays to uncover aberrant histone modifying activities in cell extracts derived from different disease states.

Acknowledgements

We thank all the members of the Denu and the Jarrard research groups for technical advice and support, especially Dr. S. Oliver and Dr. Z. Su for their intellectual contribution in the preparation and development of a peptide microarray. This work was supported by the National Institutes of Health (R01 GM065386) and U.S. Department of Defense (DOD) through PCa Research Program (W81XWH-15-1-0628). J.H.L is a recipient of an American Heart Association postdoctoral fellowship. Tissue array was contributed by Prostate Cancer Biorepository Network (PCBN) supported by the DOD PCa Research Program (W81XWH-14-2-0182, -0183, -0185, -0186, and W81XWH-15-2-0062). The authors thank the University of Wisconsin Translational Research Initiatives in Pathology laboratory for use of its facilities and services.

Author Contributions

J.H.L., D.F.J., and J.M.D. conceived and designed the study. J.H.L. developed and optimized the microarray-based enzyme assay platform, performed biochemical experiments, and analyzed protein levels. M.D.B. synthesized histone peptide and printed the peptide arrays. B.Y. prepared the PCa cell lines and performed the transcriptomic analysis of PCa cell lines and xenograft samples. N.D. analyzed human PCa cell line expression profile from GEO database repository and analyzed tissue microarray immunohistochemistry data. W.H. performed segmentation of TMA images for IHC analysis. E.C. prepared the human xenografts. J.H.L., J.M.D. and D.F.J. wrote and revised the manuscript. All authors discussed the results and commented on the manuscript.

REFERENCES

1. Oliver S, Musselman C, Srinivasan R, Svaren J, Kutateladze T, Denu J. Multivalent Recognition of Histone Tails by the PHD Fingers of CHD5. Biochemistry **2012**;51(33):6534-44 doi 10.1021/bi3006972.
2. Cheung P, Tanner KG, Cheung WL, Sassone-Corsi P, Denu JM, Allis CD. Synergistic coupling of histone H3 phosphorylation and acetylation in response to epidermal growth factor stimulation. Molecular Cell **2000**;5(6):905-15.
3. Jenuwein T, Allis C. Translating the histone code. Science **2001**;293(5532):1074-80 doi 10.1126/science.1063127.
4. Kouzarides T. Chromatin modifications and their function. Cell **2007**;128(4):693-705 doi 10.1016/j.cell.2007.02.005.
5. Esteller M. Cancer epigenomics: DNA methylomes and histone-modification maps. Nature Reviews Genetics **2007**;8(4):286-98 doi 10.1038/nrg2005.
6. Gygi SP, Rochon Y, Franza BR, Aebersold R. Correlation between protein and mRNA abundance in yeast. Molecular and Cellular Biology **1999**;19(3):1720-30.
7. LeRoy G, DiMaggio P, Chan E, Zee B, Blanco M, Bryant B*, et al.* A quantitative atlas of histone modification signatures from human cancer cells. Epigenetics & Chromatin **2013**;6 doi 10.1186/1756-8935-6-20.
8. Huang H, Lin S, Garcia B, Zhao Y. Quantitative Proteomic Analysis of Histone Modifications. Chemical Reviews **2015**;115(6):2376-418 doi 10.1021/cr500491u.
9. Vogel C, Marcotte EM. Insights into the regulation of protein abundance from proteomic and transcriptomic analyses. Nat Rev Genet **2012**;13(4):227-32 doi 10.1038/nrg3185.
10. Stitt M, Gibon Y. Why measure enzyme activities in the era of systems biology? Trends Plant Sci **2014**;19(4):256-65 doi 10.1016/j.tplants.2013.11.003.
11. Stephenson AJ, Kattan MW, Eastham JA, Bianco FJ, Jr., Yossepowitch O, Vickers AJ*, et al.* Prostate cancer-specific mortality after radical prostatectomy for patients treated in the prostate-specific antigen era. Journal of clinical oncology : official journal of the American Society of Clinical Oncology **2009**;27(26):4300-5 doi 10.1200/JCO.2008.18.2501.
12. Eisenberger MA, Carducci MA. Chemotherapy for Hormone-Resistant Prostate Cancer. Philadelphia2002.
13. Seligson DB, Horvath S, Shi T, Yu H, Tze S, Grunstein M*, et al.* Global histone modification patterns predict risk of prostate cancer recurrence. Nature **2005**;435(7046):1262-6 doi 10.1038/nature03672.
14. Bianco-Miotto T, Chiam K, Buchanan G, Jindal S, Day TK, Thomas M*, et al.* Global Levels of Specific Histone Modifications and an Epigenetic Gene Signature Predict Prostate Cancer Progression and Development. Cancer Epidemiology Biomarkers & Prevention **2010**;19(10):2611-22 doi 10.1158/1055-9965.epi-10-0555.
15. Dawson M, Prinjha R, Dittmann A, Giotopoulos G, Bantscheff M, Chan W*, et al.* Inhibition of BET recruitment to chromatin as an effective treatment for MLL-fusion leukaemia. Nature **2011**;478(7370):529-33 doi 10.1038/nature10509.
16. Fraga MF, Ballestar E, Villar-Garea A, Boix-Chornet M, Espada J, Schotta G*, et al.* Loss of acetylation at Lys16 and trimethylation at Lys20 of histone H4 is a common hallmark of human cancer. Nat Genet **2005**;37(4):391-400 doi 10.1038/ng1531.
17. Su Z, Boersma MD, Lee JH, Oliver SS, Liu S, Garcia BA*, et al.* ChIP-less analysis of chromatin states. Epigenetics Chromatin **2014**;7:7 doi 10.1186/1756-8935-7-7.
18. Britton L, Gonzales-Cope M, Zee B, Garcia B. Breaking the histone code with quantitative mass spectrometry. Expert Review of Proteomics **2011**;8(5):631-43 doi 10.1586/EPR.11.47.

19. Corey E, Quinn JE, Buhler KR, Nelson PS, Macoska JA, True LD*, et al.* LuCaP 35: a new model of prostate cancer progression to androgen independence. Prostate **2003**;55(4):239-46 doi 10.1002/pros.10198.
20. Luger K, Rechsteiner TJ, Richmond TJ. Preparation of nucleosome core particle from recombinant histones. Methods Enzymol **1999**;304:3-19.
21. Berndsen C, Denu J. Assays for mechanistic investigations of protein/histone acetyltransferases. Methods **2005**;36(4):321-31 doi 10.1016/j.ymeth.2005.03.002.
22. Huang W, Hennrick K, Drew S. A colorful future of quantitative pathology: validation of Vectra technology using chromogenic multiplexed immunohistochemistry and prostate tissue microarrays. Hum Pathol **2013**;44(1):29-38 doi 10.1016/j.humpath.2012.05.009.
23. Thiele A, Stangl GI, Schutkowski M. Deciphering Enzyme Function Using Peptide Arrays. Molecular Biotechnology **2011**;49(3):283-305 doi 10.1007/s12033-011-9402-x.
24. Cretich M, Damin F, Pirri G, Chiari M. Protein and peptide arrays: Recent trends and new directions. Biomolecular Engineering **2006**;23(2-3):77-88 doi 10.1016/j.bioeng.2006.02.001.
25. Choudhary C, Weinert B, Nishida Y, Verdin E, Mann M. The growing landscape of lysine acetylation links metabolism and cell signalling. Nature Reviews Molecular Cell Biology **2014**;15(8):536-50 doi 10.1038/nrm3841.
26. Arnold KM, Lee S, Denu JM. Processing Mechanism and Substrate Selectivity of the Core NuA4 Histone Acetyltransferase Complex. Biochemistry **2011**;50(5):727-37 doi 10.1021/bi101355a.
27. Love IM, Sekaric P, Shi D, Grossman SR, Androphy EJ. The histone acetyltransferase PCAF regulates p21 transcription through stress-induced acetylation of histone H3. Cell Cycle **2012**;11(13):2458-66 doi 10.4161/cc.20864.
28. Feldman J, Dittenhafer-Reed K, Denu J. Sirtuin Catalysis and Regulation. Journal of Biological Chemistry **2012**;287(51):42419-27 doi 10.1074/jbc.R112.378877.
29. Thalmann G, Sikes R, Wu T, Degeorges A, Chang S, Ozen M*, et al.* LNCaP progression model of human prostate cancer: Androgen-independence and osseous metastasis. Prostate **2000**;44(2):91-103.
30. Thalmann GN, Anezinis PE, Chang SM, Zhau HE, Kim EE, Hopwood VL*, et al.* ANDROGEN-INDEPENDENT CANCER PROGRESSION AND BONE METASTASIS IN THE LNCAP MODEL OF HUMAN PROSTATE-CANCER. Cancer Research **1994**;54(10):2577-81.
31. Liu X, Wang L, Zhao KH, Thompson PR, Hwang Y, Marmorstein R*, et al.* The structural basis of protein acetylation by the p300/CBP transcriptional coactivator. Nature **2008**;451(7180):846-50 doi 10.1038/nature06546.
32. Thompson PR, Wang D, Wang L, Fulco M, Pediconi N, Zhang D*, et al.* Regulation of the p300 HAT domain via a novel activation loop. Nat Struct Mol Biol **2004**;11(4):308-15 doi 10.1038/nsmb740.
33. Black JC, Mosley A, Kitada T, Washburn M, Carey M. The SIRT2 deacetylase regulates autoacetylation of p300. Mol Cell **2008**;32(3):449-55 doi 10.1016/j.molcel.2008.09.018.
34. Ha S, Iqbal NJ, Mita P, Ruoff R, Gerald WL, Lepor H*, et al.* Phosphorylation of the androgen receptor by PIM1 in hormone refractory prostate cancer. Oncogene **2013**;32(34):3992-4000 doi 10.1038/onc.2012.412.
35. Debes J, Sebo T, Lohse C, Murphy L, Haugen D, Tindall D. p300 in prostate cancer proliferation and progression. Cancer Research **2003**;63(22):7638-40.
36. Karanam B, Jiang L, Wang L, Kelleher NL, Cole PA. Kinetic and mass spectrometric analysis of p300 histone acetyltransferase domain autoacetylation. J Biol Chem **2006**;281(52):40292-301 doi 10.1074/jbc.M608813200.
37. Finnin MS, Donigian JR, Pavletich NP. Structure of the histone deacetylase SIRT2. Nat Struct Biol **2001**;8(7):621-5 doi 10.1038/89668.

38. North BJ, Verdin E. Mitotic regulation of SIRT2 by cyclin-dependent kinase 1-dependent phosphorylation. Journal of Biological Chemistry **2007**;282(27):19546-55 doi 10.1074/jbc.M702990200.
39. Debes JD, Schmidt LJ, Huang HJ, Tindall DJ. p300 mediates androgen-independent transactivation of the androgen receptor by interleukin 6. Cancer Research **2002**;62(20):5632-6.
40. Han Y, Jin Y-H, Kim Y-J, Kang B-Y, Choi H-J, Kim D-W*, et al.* Acetylation of Sirt2 by p300 attenuates its deacetylase activity. Biochemical and Biophysical Research Communications **2008**;375(4):576-80 doi 10.1016/j.bbrc.2008.08.042.
41. Dryden SC, Nahhas FA, Nowak JE, Goustin AS, Tainsky MA. Role for human SIRT2 NAD-dependent deacetylase activity in control of mitotic exit in the cell cycle. Mol Cell Biol **2003**;23(9):3173-85.
42. Hiratsuka M, Inoue T, Toda T, Kimura N, Shirayoshi Y, Kamitani H*, et al.* Proteomics-based identification of differentially expressed genes in human gliomas: down-regulation of SIRT2 gene. Biochemical and Biophysical Research Communications **2003**;309(3):558-66 doi 10.1016/j.bbrc.2003.08.029.
43. Soucek K, Kamaid A, Phung AD, Kubala L, Bulinski JC, Harper RW*, et al.* Normal and prostate cancer cells display distinct molecular profiles of alpha-tubulin posttranslational modifications. Prostate **2006**;66(9):954-65 doi 10.1002/pros.20416.
44. Inoue T, Hiratsuka M, Osaki M, Yamada H, Kishimoto I, Yamaguchi S*, et al.* SIRT2, a tubulin deacetylase, acts to block the entry to chromosome condensation in response to mitotic stress. Oncogene **2007**;26(7):945-57 doi 10.1038/sj.onc.1209857.
45. Pandithage R, Lilischkis R, Harting K, Wolf A, Jedamzik B, Lüscher-Firzlaff J*, et al.* The regulation of SIRT2 function by cyclin-dependent kinases affects cell motility. J Cell Biol **2008**;180(5):915-29 doi 10.1083/jcb.200707126.
46. Inoue T, Nakayama Y, Yamada H, Li YC, Yamaguchi S, Osaki M*, et al.* SIRT2 downregulation confers resistance to microtubule inhibitors by prolonging chronic mitotic arrest. Cell Cycle **2009**;8(8):1279-91.
47. Arrowsmith CH, Bountra C, Fish PV, Lee K, Schapira M. Epigenetic protein families: a new frontier for drug discovery. Nat Rev Drug Discov **2012**;11(5):384-400 doi 10.1038/nrd3674.

FIGURE LEGENDS

Figure 1. Immunodetection of acetylated peptides during the activity assay on the histone microarray.

(A) The library used in this study consists of 932 different peptides covering human histone sequences and PTM states. A duplicate set (represented by pink and light turquoise each) of librarires allows two different reaction conditions to be probed simultaneously when used with a duplex chamber. The scheme represented here is HAT-dependent lysine acetylation monitored by an immunoassay using the anti-*pan*-K_{ac} antibody.

(B) Fluorescence signals at 532 nm come from Cy3-cellulose dye mixed with the peptide stock solution, which was used as a spot tracer (*green*), while Alexa Fluor®647 signal (*red*) that represents peptides with K_{ac} group can be monitored at 635 nm. Each peptide is printed in triplicate for statistical analysis.

(**C**) A scatter plot of signals at 532 nm and at 635 nm each respectively. Signals from each peptide in two different chambers treated with a buffer solution containing co-factors without cell lysates are compared, exhibiting high correlation and intra-array concordance.

(**D**) A Box-and-whisker plot of % signal intensity at 635 nm across the peptide library of varying number of K_{ac} (*N*). The whiskers represented the 95% confidence interval while the outliers were shown as dots. The lower and upper lines of the boxes are the quartile range with a cross line in the middle representing a median value in each *n* group. Each group represents varying number of K_{ac} per peptide (*n*) from *0* (median, $M = 8.6$, number of population, $N = 711$), *1* ($M = 30.2$, $N = 149$), *2* ($M = 56.7$, $N = 39$), 3 ($M = 72.2$, $N = 17$), or ≥4 ($M = 84.0$, $N = 13$). The differences of signal intensity between each group are statistically significant (*, $0.01 < P \leq 0.05$; **, $0.001 < P \leq 0.01$; ***, $P \leq 0.001$).

(**E**) Sirtuin assays on histone peptide microarray using peptides with acetylated lysine residues. Deacetylation activity was observed when recombinant Sirtuins (Sirt1, Sirt2 and Sirt3) were added to the assay (pink and pistachio bar). In the absence of Sirtuin as well as HEK293T cell extracts (CE), deacetylation activity is almost negligible (brown bar). Addition of CE to Sirtuin mitigated deacetylation activity (pistachio bar), while addition of CE without Sirtuin supplementation still managed to deacetylate up to 40% (dark olive bar).

(**F**) Microarray-based assay scheme used in this study for identification of HAT and Sirtuin activity.

Figure 2. Differential lysine acetylation (K_{ac}) profiles in C4-2 versus LNCaP.

(**A**) In the global HAT activity assay, cell lysates of LNCaP and C4-2 were added in presence of acetyl-coA (cofactor required for HATs activity), while TSA (HDAC inhibitor) and nicotinamide (Sirtuin inhibitor) were added to suppress HDAC and Sirtuin activity. Shown here is a snapshot taken from the same microarray after either HAT assay were performed. All the peptides were printed in triplicate with Cy3 dye as printing control and spot tracer as shown in green. The Alexa Fluor®647 signal (*red)* became more intensive when peptides with either H3K9 (peptide #32) or H3K18 (#189) residue was incubated with C4-2 in HAT activity assay when compared to with LNCaP. Peptides with pre-acetylated lysines (#926) didn't show differences in the signal. The peptides with most differential HAT activity were shown in the table in the decreasing order of K_{ac} signal. Upregulation in acetylation was observed at several lysine sites, most prominently at H3K18, H3K4, H3K9, and H3K14 sites.

(**B**) Sirtuin activity in each PCa cell line was monitored after incubation with NAD^+ cofactor, anarcardic acid (HATs inhibitor), TSA (HDAC inhibitor), and cell lysates from either LNCaP or C4-2. When peptides with pre-installed acetyllysine at either H3K9 (#103) or H3K14 (#165) were incubated with C4-2, there was less reduction in the K_{ac} fluorescent signal (i.e. higher positive signal). Higher K_{ac} signals were observed in peptides harboring acetylation at H3K9, H3K14, and H4K5/K8/K12/K16. Lower K_{ac} signals were detected at peptides with acetylation at H3K122, H3K56, and H3K4. In both acetylation and deacetylation profiles, a blue bar indicates higher K_{ac} in C4-2 (CR PCa) compared to LNCaP (HS PCa) while a red bar indicates decreased K_{ac} signal in C4-2 versus LNCaP. The column on the right represents the position of the peptide sequence within histone and the PTM mark introduced. When peptides with pre-installed acetyllysine at either H3K9 (#103) or H3K14 (#165) were incubated with C4-2 there was less reduction in the fluorescent signal.

Figure 3. Upregulation of lysine acetylation of histone H3 *N*-terminal tail in castrate-resistant C4-2.

(**A**) Lysine acetylation of histone H3 (1-20) peptide by endogenous HAT activity in C4-2 versus LNCaP as monitored by isotopic incorporation of tritium-labeled acetyl group from ^{3}H-acetyl CoA shows higher acetylation on the H3 peptide when incubated with C4-2 compared with LNCaP.

(**B**) Quantification of western blot analyses showing endogenous acetylation level at H3K9, H3K14, and H3K18 sites in LNCaP compared to C4-2. Each histone PTM was normalized against the histone H3 band ($n = 3$ for each PTM). All data represent the mean ± s.d. *, $P \leq 0.05$, and **, $P \leq 0.01$.

Figure 4. Endogenous protein and gene expression levels against HATs and Sirtuins in HS versus CR prostate cancer cell lines. (See supplementary figure, Fig S4. for the full image of the western blot used for the quantitative immunoblot analysis) For all the data shown in this figure, n > 3; *n.s.,* $P > 0.5$; *, $P \leq 0.05$; **, $P \leq 0.01$, ***, $P \leq 0.001$.

(**A**) Representative immunoblots showing the levels of HAT proteins, PCAF, Gcn5, p300, and acetyl-p300(K1499ac), normalized to α-tubulin level.

(**B**) Representative immunoblots for Sirtuin levels and quantification result for SIRT1-4, 6, and 7 in total cell extract of LNCaP versus C4-2 as normalized to α-tubulin level. Quantification of Sirt1-3 levels shows a drastic reduction in the cellular level of Sirt2 as well as Sirt3 in C4-2 Differences in the cellular level of Sirt1, Sirt4, Sirt6 and Sirt7 between the two cell lines were not significant. Sirt5 was not measured as it is reported to have no detectable deacetylase activity.

(**C**) SIRT2-dependent deacetylation of acetyl-p300(K1499ac) over time as represented by immunoblots of p300 and Ac-p300(K1499ac). The Ac-p300 band was removed in both LNCaP and C4-2 after 1 hour of incubation with SIRT2 and NAD^+. When LNCaP and C4-2 was not treated with neither NAD+ nor SIRT2,acetyl-p300 (K1499ac) level was higher in C4-2 while the p300 level was comparable between LNCaP and C4-2 cell extracts.

(**D**) Quantification result for protein levels of SIRT2 and SIRT3 in six different prostate cancer cell lines as determined by Western blots and normalized to the level of α-tubulin in the whole cell extracts. The first two cell lines are HS cell lines, LAPC4, LNCaP; and PC3, DU145, 22RV1, and C4-2 are CR cell lines.

Figure 5. Changes in the abundance of histone modifiers in HS vs. CR human prostate cancer.

(**A**) The mRNA expression has been detected by qRT-PCR. A bar graph showing SIRT2 gene expression as represented by log2 fold change of CR over HS cells. Each compared pairs are generated from the same individuals as the tissue progressed from AS to CR by serial xenografts. The numbers in the x-axis represent each patient. The bar graph is the average of three technical replicates with standard error represented by standard deviation. At least 7 xenografts exhibited SIRT2 downregulation.

(**B**) Representative staining of HS (a, b, c, g, h) and CR (d, e, f, i, j) PCa. Composite images of multiplexed staining are shown at the top panel (a, d, g, i). Spectral libraries of individual stains were used to segment composite images for quantitative analysis. The selected images demonstrate segmented stains for Sirt2 (b, e), H3K18ac (c, f), and P300 (h, j). These images are representative of the mean intensity of HS and CR PCa for each marker shown (±10% Optical Density).

(**C**) SIRT2, H3K18ac, and P300 expression in tissue microarrays containing HS and CR PCa. Box plots of the optical density (OD) of p300, H3K18ac, and Sirt2 immunohistochemistry. Each box represent 25% to 75% percentile range, solid horizontal lines represent medians, and notches represent 95% confidence intervals of the medians. Dots represent individual patient tumors in each group. Tissue and cellular segmentation of IHC staining revealed significantly increased nuclear H3K18Ac in the epithelium of CR prostate cancer samples (P = 0.013), while epithelial total Sirt2 and nuclear P300 expression did not significantly change in CR vs. HS samples.

(D) Reduction of H3K18ac level in C646-treated LNCaP and PC3 cells. At 10 μM concentration both cells showed decrease in the level of H3K18 acetylation over time as detected by the western blot analysis using anti-H3K18ac antibody. Three replicate experiment was averaged and represented with s.d. The significance of the values were shown using standard convention of $p > 0.5$; *, $p \leq 0.05$; **, $p \leq 0.01$, ***, $p \leq 0.001$.

(E) Changes in the mRNA expression of AR and PSA in PCa cell lines after treatment with p300 inhibitor, C646 up to 48 h are shown. mRNA level was detected by qRT-PCR, normalized to housekeeping gene GAPDH, and represented as relative expression to control expression. Overall, both AR and PSA showed higher expression after C646 treatment in Du145 cell lines, while LNCaP did not show significant changes compared to control experiment.

FIGURES AND TABLES

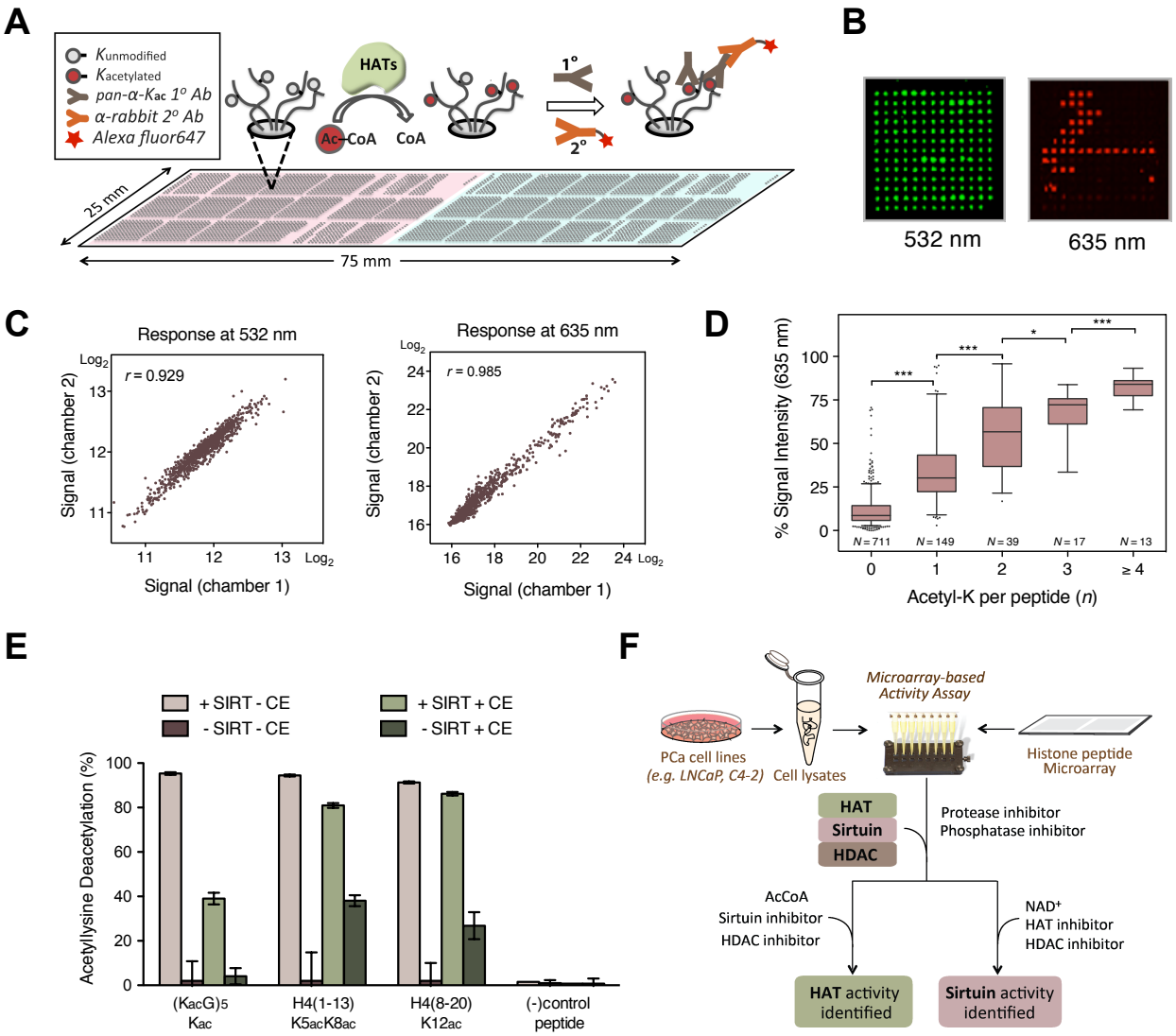

Figure 1. Immunodetection of acetylated peptides during the activity assay on the histone microarray.

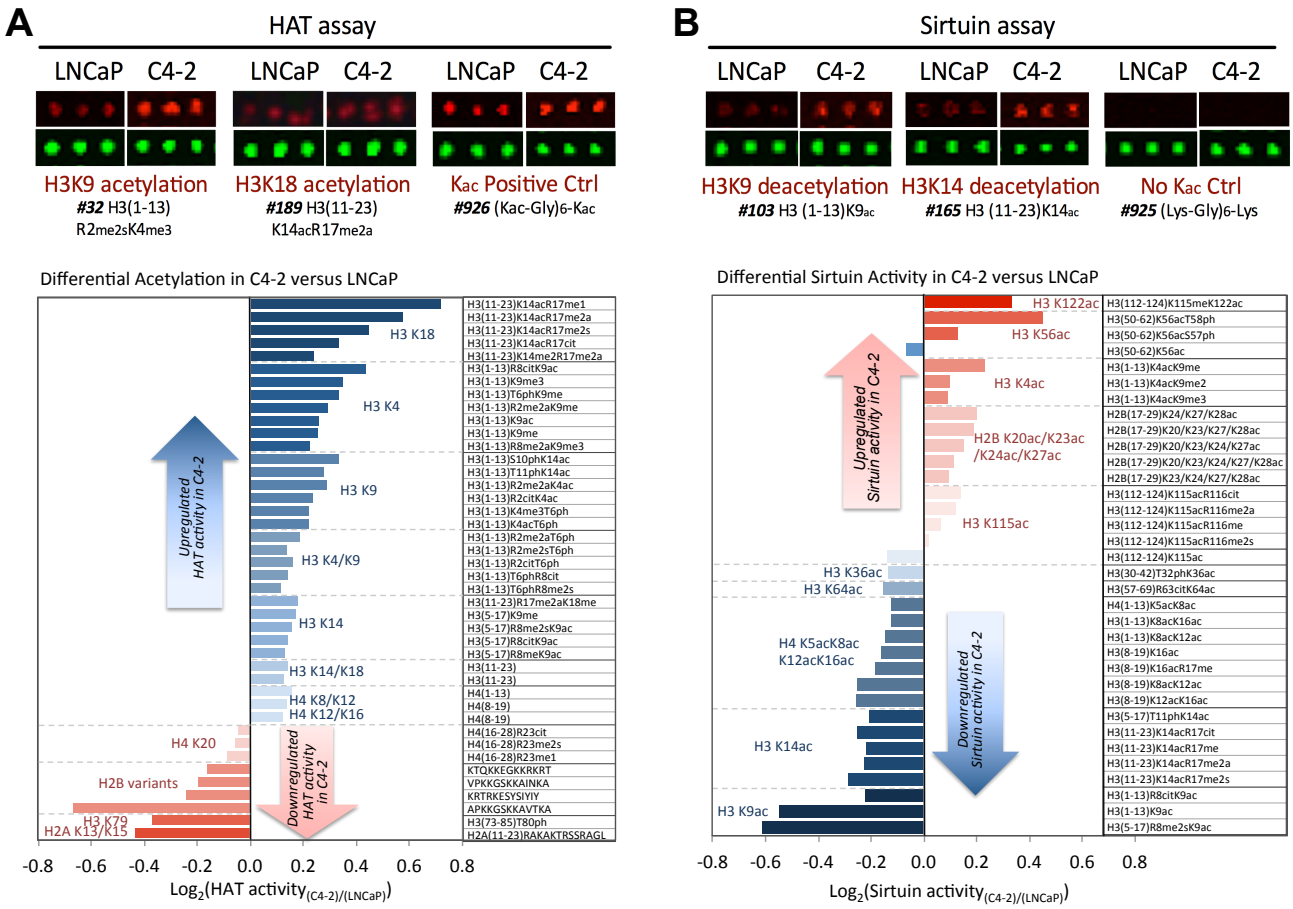

Figure 2. Differential lysine acetylation (K_{ac}) profiles in C4-2 versus LNCaP.

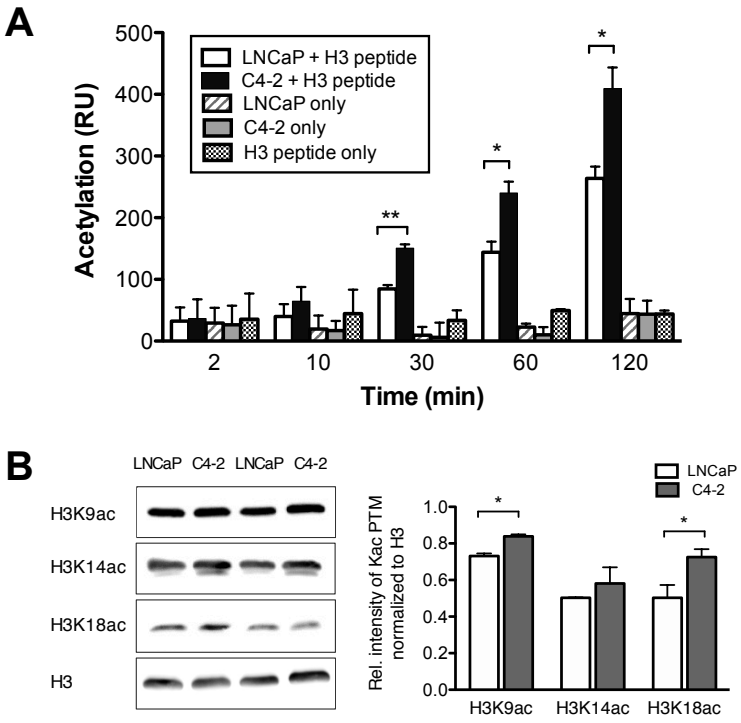

Figure 3. Upregulation of lysine acetylation of histone H3 *N*-terminal tail in castrate-resistant C4-2.

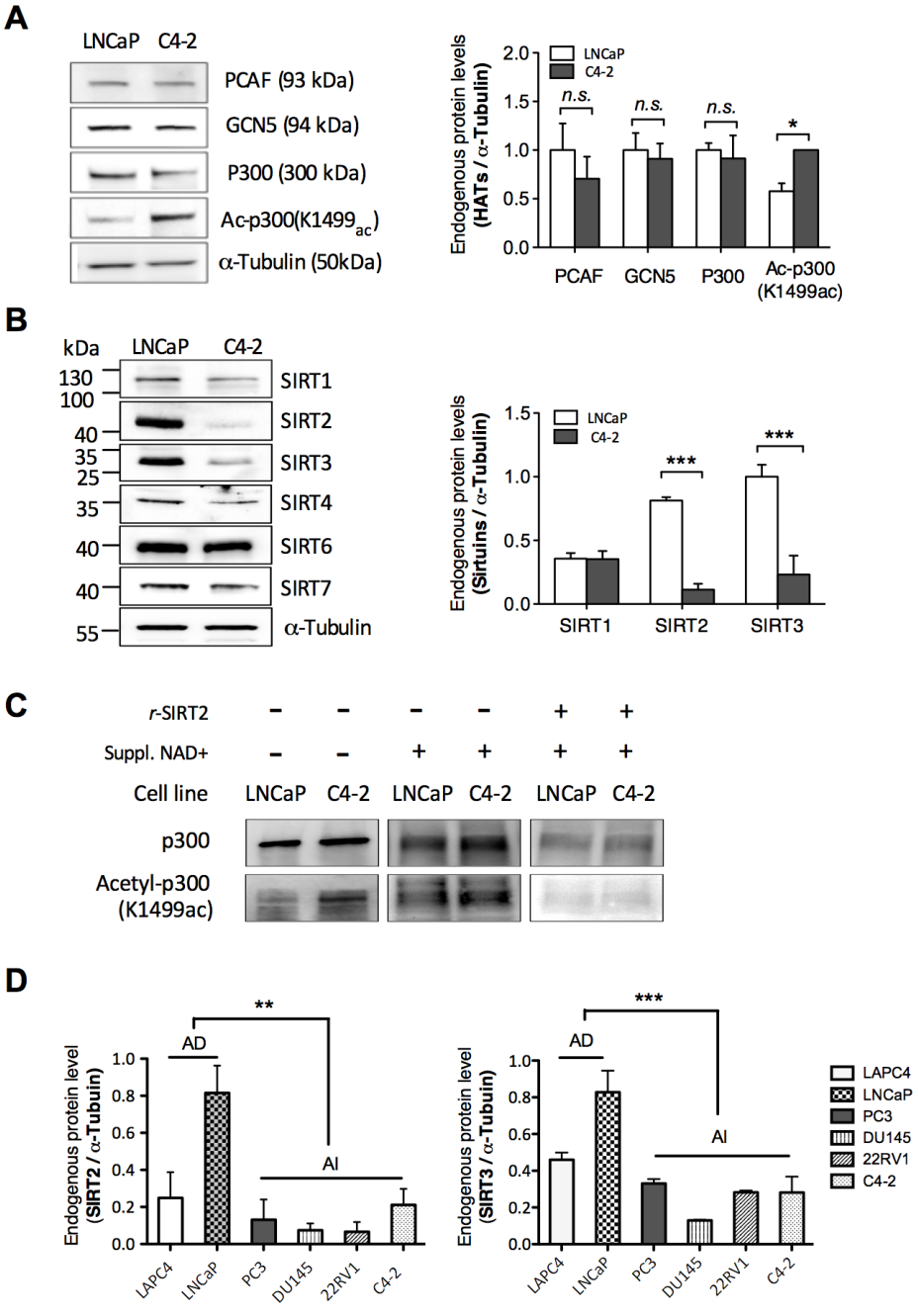

Figure 4. Endogenous protein and gene expression levels against HATs and Sirtuins in HS versus CR prostate cancer cell lines.

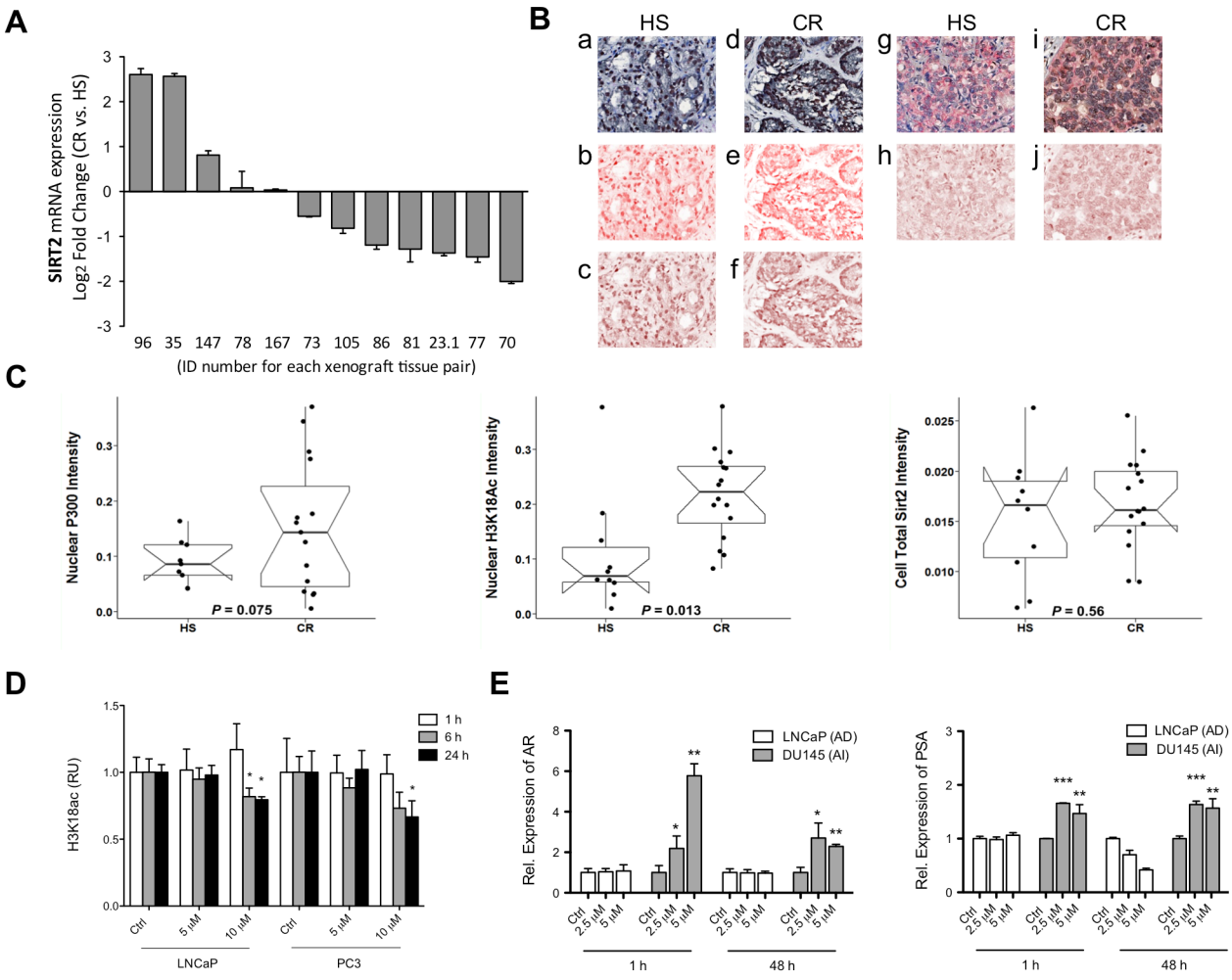

Figure 5. Changes in the abundance of histone modifiers in HS vs. CR human prostate cancer.